bioRxiv preprint doi: https://doi.org/10.1101/2022.11.14.516465; this version posted November 15, 2022. The copyright holder for this preprint (which was not certified by peer review) is the author/funder, who has granted bioRxiv a license to display the preprint in perpetuity. It is made available under aCC-BY-ND 4.0 International license.

Neuroanatomical substrates in Parkinson's Disease psychosis and their association with serotonergic receptor gene expression: A coordinate-based meta-regression analysis

Sara Pisani, MSc, [1], Brandon Gunasekera, MSc, [1], Yining Lu, MSc [2], Miriam Vignando, PhD, [3], Dominic ffytche, MD, PhD, [4], Dag Aarsland, MD, PhD, [4,5], K. Ray Chaudhuri, MD, FRCP, DSc [6], Clive Ballard, MD, [7], Jee-Young Lee, MD, PhD, [8], Yu Kyeong Kim, MD, PhD, [9], Latha Velayudhan, MD, [4^], Sagnik Bhattacharyya, MD, PhD, [1^] *

Author affiliations:

[1] Division of Academic Psychiatry, Department of Psychosis Studies, Institute of Psychiatry, Psychology and Neuroscience, King's College London, London, SE5 8AF, United Kingdom

[2] Department of Psychological Medicine, Institute of Psychiatry, Psychology and Neuroscience, King's College London, London, SE5 8AF, United Kingdom

[3] Centre for Neuroimaging Science, Institute of Psychiatry, Psychology and Neuroscience, King's College London, London, SE5 8AF, United Kingdom

[4] Division of Academic Psychiatry, Department of Old Age Psychiatry, Institute of Psychiatry, Psychology and Neuroscience, King's College London, London, SE5 8AF, United Kingdom

[5] Centre for Age-Related Medicine (SESAM), Stavanger University Hospital, Stavanger, Norway

[6] Department of Neurosciences, Institute of Psychiatry, Psychology and Neuroscience, and Parkinson's Foundation Centre of Excellence, King's College Hospital, London, United Kingdom

[7] Medical School, Medical School Building, St Luke's Campus, Magdalen Road, University of Exeter, Exeter, EX1 2LU, United Kingdom

[8] Department of Neurology, Seoul National University-Seoul Metropolitan Government, Boramae Medical Center, 20, Boramae-ro 5-gil, Dongjak-gu, Seoul 07061, Republic of Korea

[9] Department of Nuclear Medicine, Seoul National University-Seoul Metropolitan Government, Boramae Medical Center, 20, Boramae-ro 5-gil, Dongjak-gu, Seoul 07061, Republic of Korea

^ Joint Senior Authors

bioRxiv preprint doi: https://doi.org/10.1101/2022.11.14.516465; this version posted November 15, 2022. The copyright holder for this preprint (which was not certified by peer review) is the author/funder, who has granted bioRxiv a license to display the preprint in perpetuity. It is made available under aCC-BY-ND 4.0 International license.

*Corresponding author and address for reprints:

Professor Sagnik Bhattacharyya
Department of Psychosis Studies, Box P067
Institute of Psychiatry, Psychology & Neuroscience,
De Crespigny Park, London SE5 8AF, UK
Tel: +44(0)20 7848 0955
Fax: +44(0)20 7848 0976
Email: sagnik.2.bhattacharyya@kcl.ac.uk

ORCID

Sara Pisani	0000-0001-8532-4650
Brandon Gunasekera	0000-0003-1920-9376
Yining Lu	Not applicable
Miriam Vignando	0000-0002-7542-3089
Dominic ffytche	0000-0002-4214-9642
Dag Aarsland	0000-0001-6314-216X
K. Ray Chaudhuri	0000-0003-2815-0505
Clive Ballard	0000-0003-0022-5632
Jee-Young Lee	0000-0002-9120-2075
Yu Kyeong Kim	0000-0002-3282-822X
Latha Velayudhan	0000-0002-7712-930X
Sagnik Bhattacharyya	0000-0002-8688-8025

Word count (excluding abstract, tables and reference list): 4672

Word count (abstract): 236

Running head: Neuroanatomical substrates in PD psychosis

Conflict of interest: The authors have declared that no competing interests exist.

Funding: SB, LV, DA, DF, KRC and CB are in receipt of funding from Parkinson's UK for a clinical trial in Parkinson's disease psychosis. SP PhD studentship is funded by Parkinson's UK. The funding source had no involvement in this research. SB is supported by grants from the National Institute of Health Research (NIHR) Efficacy and Mechanism Evaluation scheme and Parkinson's UK. SB has participated in advisory boards for or received honoraria as a speaker from Reckitt Benckiser, EmpowerPharm/SanteCannabis and Britannia Pharmaceuticals. All of these honoraria were received as contributions toward research support through King's College London, and not personally. SB also has collaborated with Beckley

bioRxiv preprint doi: https://doi.org/10.1101/2022.11.14.516465; this version posted November 15, 2022. The copyright holder for this preprint (which was not certified by peer review) is the author/funder, who has granted bioRxiv a license to display the preprint in perpetuity. It is made available under aCC-BY-ND 4.0 International license.

Canopy Therapeutics/ Canopy Growth (investigator-initiated research) wherein they supplied study drug for free for charity (Parkinson's UK) and NIHR (BRC) funded research. The views expressed are those of the authors and not necessarily those of the NHS, the NIHR or the Department of Health. LV has collaborated with Beckley Canopy Therapeutics/ Canopy Growth (investigator-initiated research) wherein they supplied study drug for free for charity (Parkinson's UK) and NIHR (BRC) funded research.

bioRxiv preprint doi: https://doi.org/10.1101/2022.11.14.516465; this version posted November 15, 2022. The copyright holder for this preprint (which was not certified by peer review) is the author/funder, who has granted bioRxiv a license to display the preprint in perpetuity. It is made available under aCC-BY-ND 4.0 International license.

Abstract

Background: Common neural underpinning of Parkinson's Disease (PD) psychosis across different structural magnetic resonance imaging (MRI) studies remains unclear to this day with few studies and even fewer meta-analyses available.

Objectives: Our meta-analysis aimed to identify and summarise studies using MRI approach to identify PD psychosis-specific brain regions and examine the relation between cortical volume loss and dopaminergic and serotonergic receptor density.

Methods: PubMed, Web of Science and Embase were searched for MRI studies of PD psychosis (PDP) compared to PD patients without psychosis (PDnP). Seed-based *d* Mapping with Permutation of Subject Images was applied in the meta-analysis where coordinates were available. Multiple linear regressions to examine the relationship between grey matter volume loss in PDP and receptor gene expression density (extracted from the Allen Human Brain Atlas) were conducted in R.

Results: We observed lower grey matter volume in parietal-temporo-occipital regions from our meta-analysis (N studies =10, PDP n=211, PDnP, n=298). These results remained significant after adjusting for PD medications and for cognitive scores. Grey matter volume loss in PDP was associated with local expression of 5-HT1a (b=0.109, p=0.012) and 5-HT2a receptors (b=-0.106, p=0.002) also after adjusting for PD medications (5-HT1a, p = 0.005; 5-HT2a, p = 0.001).

Conclusions: Widespread cortical volume loss in the parieto-temporo-occipital regions involved in information processing and integration, as well as attention, could result in PD psychosis symptoms. Neurobiological mechanisms implicating serotonergic receptors may also contribute to this condition.

Keywords: Parkinson's disease, psychosis, neuroanatomical correlates, meta-analysis, regional receptor density

bioRxiv preprint doi: https://doi.org/10.1101/2022.11.14.516465; this version posted November 15, 2022. The copyright holder for this preprint (which was not certified by peer review) is the author/funder, who has granted bioRxiv a license to display the preprint in perpetuity. It is made available under aCC-BY-ND 4.0 International license.

1.Introduction

Non-motor symptoms of Parkinson's Disease (PD) are distressing, debilitating, and associated with poor quality of life in PD patients. Specifically, hallucinations and delusions, the key manifestations of PD psychosis (PDP), negatively impact patients and caregivers and increase care burden and risk of hospitalisation (Aarsland et al., 2007; Martinez-Martin et al., 2015). Although initially considered a by-product of dopamine augmentation treatments, evidence suggests that drug-naïve PD patients may also experience psychosis symptoms (Friedman, 2016; Pagonabarraga et al., 2016). Severity and duration of PD, dopaminergic medications, sleep disorders, cognitive decline, widespread Lewy Body pathology, and late PD onset can be risk factors for developing psychosis symptoms (Barrett et al., 2018; Chang & Fox, 2016; Factor et al., 2014; Ffytche et al., 2017; Williams & Lees, 2005).

The mechanisms underlying the emergence of psychotic symptoms in PD remain unclear. Results from structural as well as task-based and resting state magnetic resonance imaging (MRI) and positron emission tomography (PET) studies have generally reported grey matter reductions (Bejr-Kasem et al., 2019; Gama et al., 2014; Nishio et al., 2018; Ramírez-Ruiz et al., 2007) encompassing the ventral and dorsal visual pathways and hippocampus (Alzahrani & Venneri, 2015; Lenka et al., 2015; Yao et al., 2016) as well as altered temporo-parieto-occipital activation, metabolism or functional and structural connectivity in large-scale brain networks (Boecker et al., 2007; Hall et al., 2019; Hepp et al., 2017; Lefebvre et al., 2016; Shine, Halliday, et al., 2014; Shine et al., 2015; Stebbins et al., 2004). This is consistent with a recent meta-analytic synthesis reporting fronto-temporo-parieto-occipital brain grey matter reduction in a mixed group of participants with PD and Lewy body dementia (DLB) with visual hallucinations (Pezzoli et al., 2021), although they did not consider the effect of potential confounders such as PD medication or concomitant symptoms, e.g., cognitive decline. Complementing this, a recent mega-analysis (Vignando et al., 2021) has reported extensive reduction of whole-brain cortical thickness and surface areas in visual cortex, left insula and hippocampus in PD patients with visual hallucinations compared to those without, as well as a relationship between cortical thickness loss and higher regional availability serotonergic (5-HT2a and 5-HT1a) and dopaminergic receptors (D2/D3). Collectively, these reviews focused on related different metrics of brain structure (volume, cortical thickness and surface). Meta-analyses integrating evidence regarding alterations in brain areas in PD psychosis may help unravel neuroanatomical substrates underpinning Parkinson's psychosis. Here, we have conducted a quantitative analysis of structural neuroimaging studies investigating the neural

bioRxiv preprint doi: https://doi.org/10.1101/2022.11.14.516465; this version posted November 15, 2022. The copyright holder for this preprint (which was not certified by peer review) is the author/funder, who has granted bioRxiv a license to display the preprint in perpetuity. It is made available under aCC-BY-ND 4.0 International license.

correlates of psychosis in PD. Further, we examined whether the spatial distribution of brain structure alteration was associated with the spatial architecture of brain expression of the genes for dopaminergic (D1 and D2) and serotonergic receptors (namely 5-HT2a and 5-HT1a), the key candidate pathways implicated in PD psychosis (Hacksell et al., 2014). Unlike the approach adopted by Vignando et al. (2021) where they examined the relationship between the structural neuroimaging correlate and the density distribution data for each receptor of interest separately, we included the key candidate receptors of interest in a multiple regression model to allow investigation of their relationship with neuroimaging correlates after taking into account the effect of receptors belonging to other candidate pathways of interest.

2. Methods

2.1. Search strategy and eligibility criteria

We followed (PROSPERO registration number: CRD42020221904) the Preferred Reporting Items for Systematic Reviews and Meta-Analyses (PRISMA) guidelines (Moher et al., 2009) and a detailed description of the search strategy is outlined in Supplementary Material 1. Studies identified from PubMed, Web of Science, Embase and the Neurosynth database were included if they examined brain alterations associated with psychosis symptoms (i.e., hallucinations and/or delusions) after PD diagnosis using different neuroimaging modalities, and a case-control design and provided brain coordinates (or available statistical maps) in standardised reference spaces, e.g., Montreal Neurological Institute (MNI) or Talairach space. There were no exclusion or restriction for this search. For this meta-analysis, we solely focused on studies that used structural magnetic resonance imaging (MRI) modality.

2.2. Data extraction

Data extraction involved: study details (i.e., authors' names, year of publications), study design, scanner characteristics (e.g., manufacturer), sample size, sample characteristics (e.g., age, gender, education levels), PD onset age, disease duration, PD symptoms, clinical measures of psychosis symptoms, cognitive measures, dopamine-replacement medications (expressed in Levodopa equivalent daily dose (LEDD)), and other clinical outcome measures (e.g., depression). Where only median values were available, this was converted into mean (Luo et al., 2018). Coordinates type (e.g., MNI or Talairach space), and associated *t* values were also extracted. Where coordinates were expressed in Talairach or other standard normalised spaces, they were converted into MNI coordinates. Authors were contacted for studies that did not report coordinate data. Data extraction was conducted independently by two researchers (SP, YL). Discrepancies were addressed through consensus or discussion with senior researchers.

bioRxiv preprint doi: https://doi.org/10.1101/2022.11.14.516465; this version posted November 15, 2022. The copyright holder for this preprint (which was not certified by peer review) is the author/funder, who has granted bioRxiv a license to display the preprint in perpetuity. It is made available under aCC-BY-ND 4.0 International license.

2.3. Data synthesis

A coordinate-based meta-analysis was conducted for structural MRI studies reporting voxel-based morphometry (VBM) results using peak coordinates and/or statistical maps by employing a random-effects approach using Seed-based *d* Mapping with Permutating Subject Images (SDM-PSI) (version 6.21, https://www.sdmproject.com/) (Albajes-Eizagirre et al., 2019). This involved computation of upper and lower bounds of effect size maps for studies based on the available peak coordinates by imputing voxel-wise effect size (Albajes-Eizagirre et al., 2018) and combining them with statistical parametric maps provided by the studies (where applicable) converted into effect size maps to carry out a random-effects meta-analysis. Contrasts of interest were 'PD psychosis (PDP) < PD without psychosis (PDnP)' (i.e., grey matter loss) and 'PD psychosis (PDP) > PD without psychosis (PDnP)' (i.e., increased grey matter) with and without controlling for the effect of PD medications (expressed in LEDD), and cognitive scores. Due to the various neurocognitive scales used to assess cognitive abilities in PDP and PDnP patients, we computed standardised scores for each study by dividing the mean score by the standard deviation (SD) for each patients' group. Statistical parametric maps provided by the studies (where applicable) were registered to the SDM template, and their *t* values were converted into effect sizes and included in the analysis. SDM-PSI provides I^2 statistic to assess heterogeneity in the observed peaks as well as between-study heterogeneity (Higgins et al., 2003). Funnel plots for each peak and Egger's test (Egger et al., 1997) were used to assess publication bias. Clusters smaller than 10 voxels were discarded.

We examined the association between grey matter volume loss (measured using Hedges' *g* effect-size estimates extracted from the centroid of the SDM-PSI meta-analytic map parcellated across 78 brain regions of the Desikan-Killiany atlas (Desikan et al., 2006)) in PDP compared to PDnP patients with dopaminergic (D1/D2) and serotonergic (5-HT2a/5-HT1a) mRNA microarray gene expression using a multiple linear regression analysis. A secondary analysis included LEDD as a covariate when computing Hedges' g effect-size estimate. Gene expression data for dopaminergic and serotonergic receptors was extracted from the Allen Human Brain Atlas which includes microarray expression data in tissue samples from six healthy adult human brains with more than 20,000 genes quantified across cortical and subcortical regions, including brainstem and cerebellum (Hawrylycz et al., 2012). Probe-to-gene re-annotation data was downloaded using the information from Arnatkevičiūtė et al. (2019). Sample-to-region matching, and extraction of the gene expression data followed

bioRxiv preprint doi: https://doi.org/10.1101/2022.11.14.516465; this version posted November 15, 2022. The copyright holder for this preprint (which was not certified by peer review) is the author/funder, who has granted bioRxiv a license to display the preprint in perpetuity. It is made available under aCC-BY-ND 4.0 International license.

established approaches (Arnatkevičiūtė et al., 2019; Markello et al., 2021). Gene expression data for D3 receptor could not be matched to the probe and therefore was not extracted.

2.4. Quality rating assessment

Study quality was assessed with the Newcastle-Ottawa rating Scale (Wells et al., 2000) for case-control studies. This scale includes three methodological domains: "Selection" (i.e., definitions of cases and controls, and their selection), "Comparability" (i.e., comparison of cases and controls on the variables of interest, inclusion of covariates), and "Exposure" (i.e., how exposure such as condition was defined and ascertained). This rating is based on a star system: studies can be awarded a maximum of one star for each "Selection" and "Exposure" items, and a maximum of two stars for the "Comparability" domain. Quality ratings were conducted by one researcher. In this review, neural substrates of PDP patients were compared to those in PDnP patients, thus the latter acted as control or comparison group. Therefore, the items "Selection of controls" and "Definition of controls" were specifically related to PDnP patients.

3. Results

3.1. Study characteristics

Our systematic search identified 14 studies out of which 9 reported peak coordinate data, and one provided T maps (Bejr-Kasem et al., 2019; Bejr-Kasem et al., 2020; Firbank et al., 2018; Goldman et al., 2014; Lawn, 2021; Lee et al., 2017; Pagonabarraga et al., 2014; Ramírez-Ruiz et al., 2007; Shin et al., 2012; Watanabe et al., 2013). Thus, we included a total of 10 published articles (Fig. 1) reporting on a total of n= 211 PDP (mean age ± SD = 69.01 ± 4.90; motor symptom score, mean ± SD = 28.72 ± 11.69, LEDD mg/day mean ± SD = 651.9 ± 318.14) and n=298 PDnP patients (mean age ± SD = 67.34 ± 4.59, motor symptom scores, mean ± SD = 25.94 ± 8.63, LEDD mg/day mean ± SD = 577.1 ± 263.11) (Table 1).

Full quality ratings are reported in Supplementary Material 2 (eTable1). Briefly, all studies had full score on the "Exposure" domain (i.e., ascertainment, non-response rate and ascertainment method for PDP and PDnP patients); "Comparability" was good in all studies due to their matched design, whereby patients were matched on age, gender and other clinical or demographic variables, whilst other studies reported these variables as covariates in the

bioRxiv preprint doi: https://doi.org/10.1101/2022.11.14.516465; this version posted November 15, 2022. The copyright holder for this preprint (which was not certified by peer review) is the author/funder, who has granted bioRxiv a license to display the preprint in perpetuity. It is made available under aCC-BY-ND 4.0 International license.

analysis. “Selection” domain included selection and definition of both PDP patients (i.e., cases) and PDnP patients (i.e., controls), selection of PDP patients was assigned one star (i.e., the maximum) in all studies. Similarly, selection of PDnP patients was assigned one star in all studies, whilst definition of such group was clear in one study which was assigned one star in this domain.

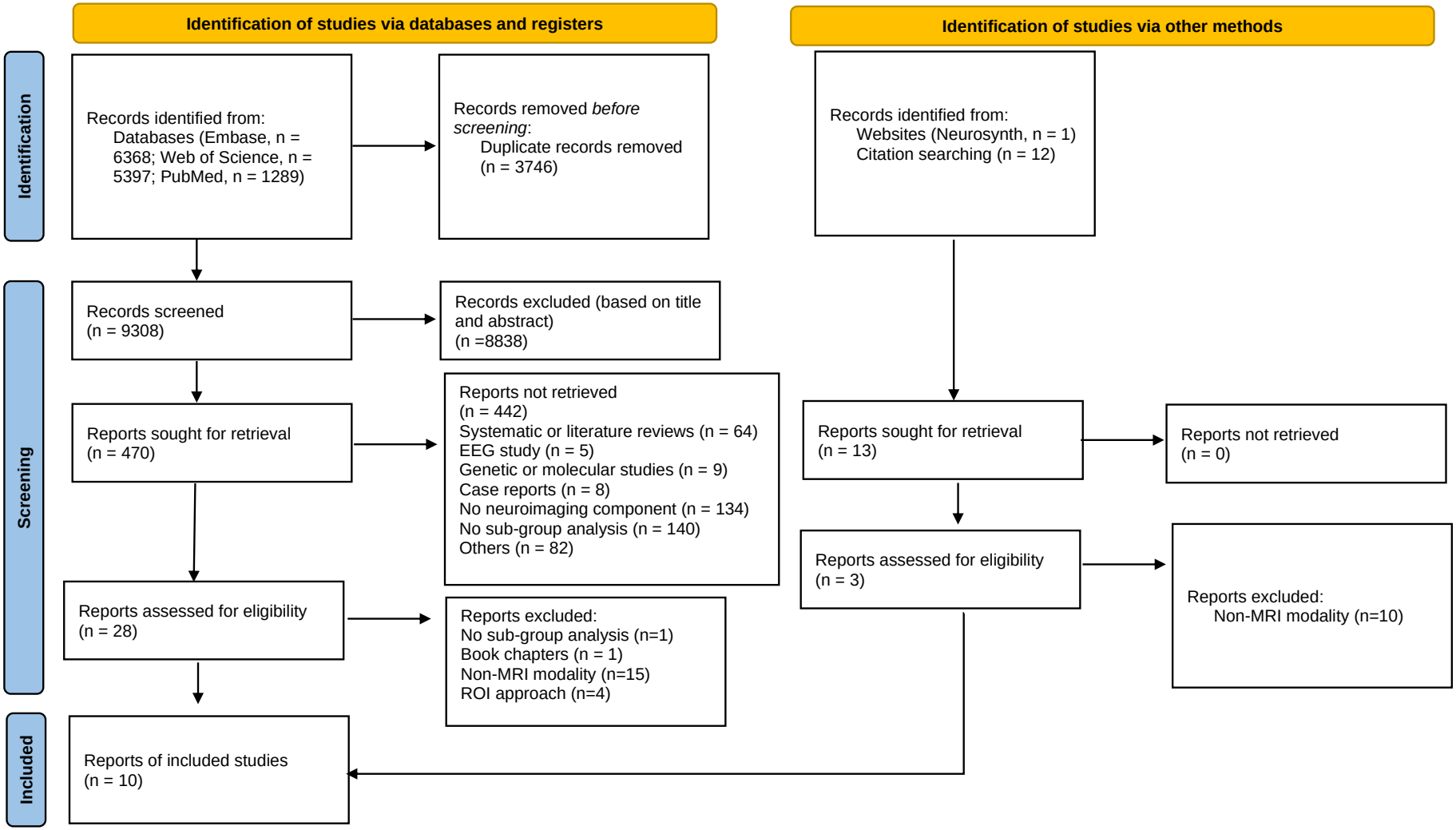

Figure 1. PRISMA flowchart showing study selection procedures.

Study	PDP patient	PDnP patients	Definition of PD psychosis	Age (mean years)	Educations (in years)	Cognitive outcome	PD onset (years)	PD duration	MDS-UPDRS part III scores (mean)	PD medications (mg/day)	Depression scores
Bejr-Kasem et al. (2019), Spain Scanner: Philips, 3.0 T	18 (10M, 8F)	14 (10M, 4F)	PD patients included if VH remained stable during the 3 months before inclusion in the study	70.4; 65.8	12.5; 11.6	PD-CRS, 91.9; 92.9	NR	5.2; 4 (years)	21.9; 25.8	LEDD 697.2 mg; 601.1 mg	HADS-D 2.2; 3.3
Lee et al. (2017), South Korea Scanner: Philips, 3.0 T	10 (7M, 3F)	21 (9M, 11F)	VH definition was based on consensus, with VH persistent for at least 3 months	69.4; 66.2	NR	MMSE 27.6; 28.2	62.2; 59.3	7.2; 7 (years)	22.5; 16.4	LEDD1031.2 mg; 805.2 mg	GDS 16.6; 15.5
Pagonabarraga et al. (2014), Spain Scanner: General Electric, 1.5 T	17 (NR)	29 (NR)	Presence of VH was assessed with the MDS-UPDRS part 1 using item 1.2	64.1; 66.3	11.1; 9.2	PD-CRS 87.2; 90.3	53.1; 58.7	9.8; 7.3 (years)	21.7; 18.6	LEDD 996 mg; 816 mg	HADS-D 5.2; 4.4
Lawn & ffytche (2021), UK Scanner: General Electric, 1.5 T	7 (3M, 4F)	9 (7M, 2F)	PD patients with a range of complex hallucinations as well as illusions, passage, and presence hallucinations	68.9; 65.1	NR	MMSE 26.9; 29.7	NR	8.71; 5.8 (years)	40; 25.6*	L-dopa n=2, L-dopa + DA n=4, DA=1; L-dopa n=2, L-dopa + DA, n=4, DA, n=3 †	
Ramirez-Ruiz et al. (2007), Spain Scanner: General Electric, 1.5 T	18 (7M, 11F)	20 (8M, 12F)	NPI (hallucination item)	NR	7.6; 7.5	MMSE 27; 29.1	NR	12.6; 10.6 (years)	29.3; 24.5	Levodopa daily dose 723.6 mg; 647.5 mg	Hamilton 6.7; 3.6
Bejr-Kasem et al. (2021), Spain Scanner: PPMI data	40 (23M, 17F)	84 (25M, 59F)	Presence of VH was assessed with the MDS-UPDRS part 1 using item 1.2	60.1; 60.7	14.5; 15.6	MoCA 27.7; 27.3	NR	7.2; 6.7 (months)	20.7; 19.8	LEDD 0 mg; 0 mg	GDS 2.1; 2.2
Watanabe et al. (2013), Japan	13 (7M, 6F)	13 (5M, 8F)	Presence of VH was assessed with	66.6; 63.6	12.7; 12.2	MMSE 27.9; 29	56.9; 53.6	10; 10 (years)	23.4; 28.6	LEDD 411.5 mg; 361 mg	BDI 21.7; 9

Scanner: Siemens, 3.0 T			the MDS-UPDRS part 1 using item 1.2								
Firbank et al. (2018), UK Scanner: Philips, 3.0 T	17 (13M, 4F)	19 (17M, 2F)	NPI (hallucination item)	75.5; 72.3	11.6; 11.1	MMSE 23.1; 25.6	NR	11; 9.6 (years)	55.9; 34.7	Levodopa in 24h 717.3 mg; 673. 5 mg	NR
Shin et al. (2012), South Korea Scanner: Philips, 3.0 T	46 (23M, 23F)	64 (26M, 38F)	Formed VH defined as "repetitive involuntary images of people, animal or objects that were experienced as real during the waking state but for which there was no objective reality", and NPI	71.3; 70.7	8.3; 8.4	MMSE 25.2; 25.7	NR	3.3; 2.8 (months)	24.1; 21.6	LEDD 482.4 mg; 501.4 mg	NR
Goldman et al. (2014), US Scanner: General Electric, 1.5 T	25 (17M, 8F)	25 (18M, 7F)	NINDS-NIMH criteria and the MDS-UPDRS part 1 using item 1.2	74.8; 75.4	15.4; 15.7	MMSE 23.9; 25.1	NR	13.1; 10.8 (years)	39; 43.5	LEDD 808.3 mg; 787.8 mg	NR

† Number of patients on PD medications

* UPDRS combined scores for part III and IV

BDI: Beck Depression Inventory; GDS: Geriatric Depression Scale; HADS-D: Hospital Anxiety and Depression Scale – depression item; LEDD: Levodopa equivalent daily dose; MDS-UPDRS: Movement Disorder Society – Unified Parkinson's Disease Rating Scale; MMSE: Mini-Mental State Examination; MoCA: Montreal Cognitive Assessment; NINDS-NIMH: National Institute of Neurological Disorders and Stroke – National Institute of Mental Health; NPI: Neuropsychiatry Inventory; NR: None reported; PD-CRS: Parkinson's Disease – Cognitive Rating Scale; VH: Visual hallucinations.

Table 1. Study description with statistics (mean, unless otherwise specified) presented for each patient group (PDP patients; PDnP patients). Number of patients for each group are presented alongside gender (males, M; females, F), years of education, scores on cognitive outcomes. Clinical variables of interest are also reported, e.g., motor symptoms (according to the MDS-UPDRS), PD medications (expressed in mean daily mg where available), and depression scores where available.

bioRxiv preprint doi: https://doi.org/10.1101/2022.11.14.516465; this version posted November 15, 2022. The copyright holder for this preprint (which was not certified by peer review) is the author/funder, who has granted bioRxiv a license to display the preprint in perpetuity. It is made available under aCC-BY-ND 4.0 International license.

3.2. Meta-analysis: Voxel-based morphometry (VBM)

Meta-analysis of 10 MRI studies (one provided statistical maps (Lee et al., 2017)) showed that PDP patients had reduced grey matter volume in parietal-temporo-occipital areas compared to PDnP patients with the largest clusters located in the right precuneus (extending to left precuneus and bilateral cuneus; voxel number = 1059, Z=-2.990, p = 0.001), bilateral inferior parietal gyrus (left inferior parietal gyrus, extending to left angular gyrus and supramarginal gyrus; voxel number = 296, Z=-2.449, p = 0.007; right inferior parietal gyrus, extending to right angular gyrus; voxel number = 277, Z=-2.225, p = 0.013), left inferior occipital gyrus (voxel number = 262, Z =-2.627, p =0.004), and right middle temporal gyrus (extending to right inferior temporal gyrus; voxel number = 225, Z = -2.664, p = 0.003) (eFigure1, Supplementary Material 3). We did not observe any significant peaks in the opposite direction (i.e., 'PDP > PDnP'). Neither between-study heterogeneity as a proportion of total variability (all I^2 statistic <25%, except right inferior parietal gyrus, which was ~27.6%) nor publication bias was observed in these peaks (Funnel plots in Supplementary Material 3). However, none of these brain regions survived correction for multiple testing. After including PD medication dose, expressed LEDD, as a covariate, grey matter reduction in right precuneus remained significant in PDP patients compared to PDnP patients (extending to left precuneus, and bilateral cuneus; voxel number = 1084, Z = -2.952, p = 0.001). There was substantial overlap between previously identified peaks, with the largest clusters in the left angular gyrus (extending to left inferior parietal gyrus; voxel number = 389, Z=-2.596, p = 0.004), right inferior temporal gyrus (extending to right middle temporal gyrus and right fusiform; voxel number = 353, Z =-.2921, p = 0.001), the left middle occipital gyrus (extending to inferior occipital gyrus; voxel number = 315, Z=-2.902, p = 0.001), and the right inferior parietal gyrus (extending to right angular gyrus; voxel number = 304, Z=-2.525, p = 0.005) (eFigure2, Supplementary Material 3). No publication bias was observed in any of these analyses (Funnel plots in Supplementary Material 3). However, none of these brain regions survived correction for multiple testing. When cognitive scores were entered as covariate, the right precuneus remained the largest cluster showing grey matter volume reduction (extending to the left precuneus, bilateral cuneus, voxel number = 1186, Z = -3.287, p < 0.001). In addition, this analysis showed other areas of lower grey matter volume in PDP compared to PDnP patients were observed. These were the left inferior occipital gyrus (extending to the middle occipital gyrus and left optic radiation, voxel number = 252, Z = -2.508, p = 0.006), the left postcentral gyrus (extending to the left precuneus, voxel number = 116, Z = -2.358, p = 0.009), and the

bioRxiv preprint doi: https://doi.org/10.1101/2022.11.14.516465; this version posted November 15, 2022. The copyright holder for this preprint (which was not certified by peer review) is the author/funder, who has granted bioRxiv a license to display the preprint in perpetuity. It is made available under aCC-BY-ND 4.0 International license.

right superior parietal gyrus (voxel number = 28, Z = -2.030, p = 0.021) (eFigure3, Supplementary Material 3). No publication bias was observed in any of these analyses (Funnel plots in Supplementary Material 3). The overlap between brain regions across the unadjusted and adjusted analyses is shown in Figure 2, and Table 2 reports peaks coordinates from the three analyses. We did not observe any significant peak in the opposite direction (i.e., 'PDP > PDnP') in either LEDD- or cognitive score-adjusted analyses. None of the areas across the three analyses survived familywise error correction.

Peak regions	MNI coordinates			Number of voxels	Z score	p value	I^2	Egger's test *p* value
	x	y	z					
PDP < PDnP								
Right precuneus (extending to left precuneus, bilateral cuneus)	10	-66	42	1059	-2.990	0.001	1.729%	n.s.
Left inferior parietal gyrus (extending to the left angular gyrus, and supramarginal gyrus)	-48	-52	40	296	-2.449	0.007	0.849%	n.s
Right inferior parietal gyrus (extending to right angular gyrus)	46	-56	44	277	-2.225	0.013	27.631%	n.s
Left inferior occipital gyrus	-38	-84	-8	262	-2.627	0.004	11.411%	n.s
Right middle temporal gyrus (extending to right inferior temporal gyrus)	52	-2	-30	225	-2.664	0.003	9.657%	n.s
Right cerebellum, hemispheric lobule VIII (extending to lobule IX)	18	-52	-54	92	-1.983	0.023	16.551%	n.s
Left median cingulate / paracingulate gyrus (extending to the right median cingulate and paracingulate gyrus)	-4	-8	46	57	-2.032	0.021	5.906%	n.s
Left inferior temporal gyrus	-46	-8	-32	42	-1.989	0.023	0.517%	n.s
Right supramarginal gyrus	58	-38	30	32	-2.179	0.014	8.127%	n.s.
Right lingual gyrus (extending to the calcarine fissure)	10	-54	8	29	-2.186	0.014	1.229%	n.s
Left postcentral gyrus (extending to left inferior parietal gyrus)	-40	-36	44	22	-2.163	0.015	5.246%	n.s
PDP < PDnP (with LEDD as covariate)								
Right precuneus (extending to the left precuneus and bilateral cuneus)	6	-62	46	1084	-2.952	0.001	5.656%	n.s.
Left angular gyrus (extending to left inferior parietal gyrus)	-50	-56	34	389	-2.596	0.004	2.443%	n.s.

	Right inferior temporal gyrus (extending to the right middle temporal gyrus and right fusiform)	50	-10	-30	353	-2.921	0.001	3.859%	n.s.
	Left middle occipital gyrus (extending to the inferior occipital gyrus)	-34	-84	6	315	-2.902	0.001	1.279%	n.s.
	Right inferior parietal gyrus (extending to the right angular gyrus)	40	-56	48	304	-2.525	0.005	3.747%	n.s
	Left median cingulate/paracingulate gyrus (extending to the right median cingulate/paracingulate gyrus and left supplementary motor area)	2	12	41	144	-2.206	0.013	2.152	n.s
	Right supramarginal gyrus	56	-40	28	117	-.2693	0.003	3.343%	n.s.
	Right lingual gyrus (extending to cerebellum, vermis lobule IV/V)	10	-52	6	105	-2.345	0.009	1.418%	n.s
	Right middle occipital gyrus	44	-76	8	104	-2.203	0.013	0.968%	n.s
	Left inferior temporal gyrus	-46	-10	-26	95	-2.270	0.011	0.526%	n.s
	Right fusiform gyrus (extending to the right cerebellum, hemispheric lobule IV/V)	24	-36	-22	85	-2.275	0.011	8.312	n.s
	Left temporal pole	-44	8	-40	47	-2.340	0.009	0.196%	n.s
	Left inferior parietal gyrus (extending to the left postcentral gyrus)	-38	-38	44	39	-2.538	0.005	7.669%	n.s
	Left cerebellum hemispheric lobule VI (extending to the left lingual gyrus)	-10	-78	-16	39	-2.197	0.014	3.506%	n.s
	Left supplementary motor area (extending to the left median cingulate/paracingulate gyrus)	-4	-12	48	26	-2.233	0.012	2.144%	n.s
	Right calcarine fissure (extending to the right lingual gyrus)	10	-86	-2	21	-2.082	0.019	0.047%	n.s
PDP < PDnP (with cognitive scores as covariate)									
	Right precuneus (extending to left precuneus, bilateral cuneus)	8	-64	38	1186	-3.287	<0.001	0.002%	n.s.
	Left inferior parietal gyrus (extending to the left angular gyrus)	-48	-52	38	467	-2.666	0.003	0.001%	n.s

	Right inferior temporal gyrus (extending to the right middle temporal gyrus)	52	-6	-30	304	-3.010	0.001	0.017%	n.s.
	Right inferior parietal gyrus (extending to right angular gyrus)	44	-58	44	280	-2.966	0.001	0.010%	n.s
	Left inferior occipital gyrus (extending to the left middle occipital gyrus)	-38	-86	-10	252	-2.508	0.006	0.002%	n.s
	Right lingual gyrus (extending to the cerebellum, vermic lobule IV/V and VI and to the right precuneus)	10	-54	6	234	-2.483	0.006	0.001%	n.s.
	Left postcentral gyrus (extending to the left precuneus, and left superior parietal gyrus)	-20	-42	66	116	-2.358	0.009	0.000%	n.s.
	Left inferior temporal gyrus (extending to the left middle temporal gyrus)	-44	-8	-30	86	-2.344	0.009	0.002%	n.s.
	Left median cingulate/paracingulate gyri (extending to the right median cingulate/paracingulate gyri)	-2	-4	42	60	-2.149	0.016	0.001%	n.s.
	Right superior parietal gyrus	26	-62	58	28	-2.030	0.021	0.002%	n.s.
	Right fusiform gyrus	30	-42	-18	17	-1.794	0.036	0.117%	n.s.

n.s.: non-significant

Table 2. Peak coordinates showing greater grey matter loss in PDP patients compared to PDnP patients, alongside number of voxels, Z scores, and associated *p* value (uncorrected), I^2 (which indicates the magnitude of between-study heterogeneity as a proportion of total variability within each peak), and publication bias expressed as Egger's test *p* value.

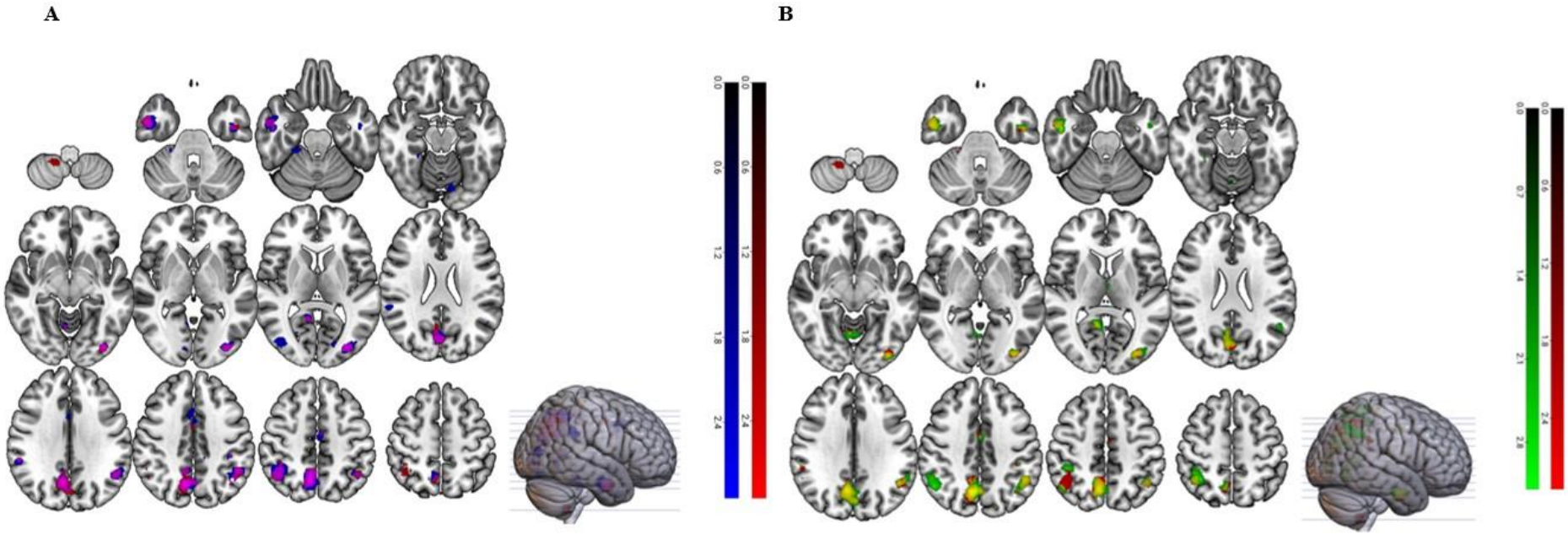

Figure 2. A) Overlapping peak areas (shown in purple) with grey matter loss in PD psychosis patients unadjusted (red) and adjusted for LEDD (expressed in mg/day) (blue) as covariate (uncorrected). This is indicated by the red and blue colour bars on which represent the T threshold of the voxels within the map. B) Overlapping peak areas (shown in yellow) with grey matter loss in PD psychosis patients unadjusted (red) and adjusted for cognitive scores (green) as covariate (uncorrected). This is indicated by the red and green colours bar on the right-hand side of the figure which represent the T threshold of the voxels within the map. The left side of the brain is shown on the right side of these brain images.

bioRxiv preprint doi: https://doi.org/10.1101/2022.11.14.516465; this version posted November 15, 2022. The copyright holder for this preprint (which was not certified by peer review) is the author/funder, who has granted bioRxiv a license to display the preprint in perpetuity. It is made available under aCC-BY-ND 4.0 International license.

3.3. Whole brain correlations with D1/D2 and 5-HT2a/5-HT1a gene expressions

Due to presence of multicollinearity in the multiple linear regression model, D2 receptor data were dropped from the analysis (i.e., due to a variation inflation factor, VIF = 6.5). Multiple linear regression analysis showed a significant association between Hedges' *g* effect-size estimates of grey matter volume unadjusted for LEDD and 5-HT2a gene expression (regression coefficient =-0.107 (95% CI, -0.174, -0.039), t=-3.147, $p = 0.002$) and 5-HT1a gene expression (regression coefficient = 0.109 (95% CI, 0.024, 0.193), t = 2.565, $p = 0.012$) but not with D1 gene expression (D1, $p = 0.554$) across the 78 regions of the Desikan-Killiany atlas. Separate analysis with Hedges' *g* effect-size estimates for grey matter volume adjusted for LEDD did not change the result (5-HT2a, regression coefficient =-0.120, 95% CI -0.190, -0.050, t=-3.408, p=0.001; 5-HT1a, regression coefficient =0.126, 95% CI 0.038, 0.213, t=2.848, p=0.006; D1, p=0.597). Presence of multicollinearity was also detected in this model and D2 was removed (VIF=6.67). Figure 3 reports the association between grey matter volume loss and receptor density from the LEDD-adjusted analysis. In both multiple linear regression models (adjusted and unadjusted for LEDD), the associations between regional cortical volume and serotonergic gene expressions were consistent in terms of direction of relationship. However, these associations were in opposite directions for the two serotonergic receptors, whereby the less the grey matter volume the more the 5-HT2a gene expression density and the less the 5-HT1a gene expression density across the 78 regions of the Desikan-Killiany atlas. That is, the greater the grey matter reduction the greater the 5-HT2a and the lower 5-HT1a gene expression density. Figures showing the relationship between cortical and subcortical spatial gene expressions and Hedges' *g* effect sizes unadjusted for LEDD are in Supplementary Material 4 (eFigure4-5).

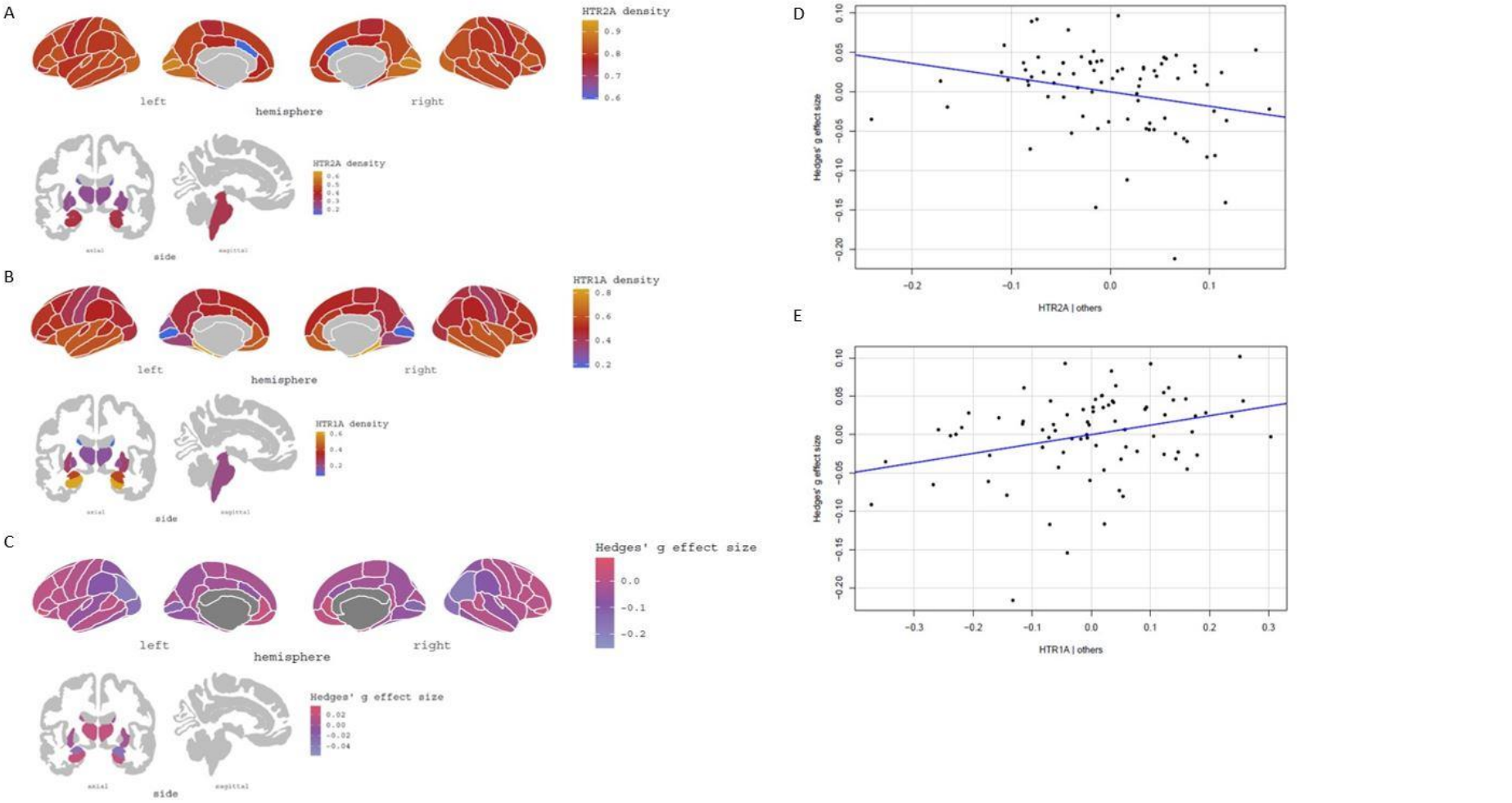

Figure 3 Gene expression density of 5-HT2a (A), 5-HT1a (B) receptors in cortical and subcortical regions, and Hedges' g effect size in cortical and subcortical regions (C) derived from the covariate meta-analysis (adjusted for LEDD) results showing decreased grey matter in PDP patients compared to PDnP patients (PDP < PDnP), parcellated across the 78 brain regions of the Desikan-Killiany atlas (Desikan et al., 2006). On the right-hand side, scatterplots showing the relationship between 5-HT2a (D) and 5-HT1a (E) with Hedges' g effect-size estimates of grey matter volume adjusted for LEDD in PDP patients compared to PDnP patients (the regression lines are adjusted for all the predictors).

bioRxiv preprint doi: https://doi.org/10.1101/2022.11.14.516465; this version posted November 15, 2022. The copyright holder for this preprint (which was not certified by peer review) is the author/funder, who has granted bioRxiv a license to display the preprint in perpetuity. It is made available under aCC-BY-ND 4.0 International license.

4. Discussion

Findings from individual studies reported extensive areas of lower grey matter volume in PDP without providing clear understanding on whether PDP may be due to structural issues in key regions or diffused anomalies. Here, we have addressed this ambiguity by incorporating results from structural MRI studies using a quantitative approach to identify neuroanatomical correlates implicated in PDP. The meta-analytic results found widespread grey matter volume reduction across parietal-temporal-occipital regions in PDP patients, specifically, the right precuneus (extending to the left precuneus), bilateral inferior parietal gyrus, and left inferior occipital gyrus, corroborating previous evidence (Goldman et al., 2014; Lenka et al., 2015; Yao et al., 2014). Volume reduction in right precuneus, bilateral inferior parietal gyrus, left median cingulate/paracingulate cortex, and right inferior and middle temporal gyrus remained significant and was independent of PD medications and cognitive scores. When PD medications and cognitive scores standardised across studies were included as a covariate, there were additional areas of lower cortical volume within occipital (e.g., left middle occipital gyrus), parietal (e.g., right lingual and left angular gyrus), and temporal regions (e.g., right fusiform gyrus). These results also extend on previous evidence (Bejr-Kasem et al., 2019; Jia et al., 2019; Lenka et al., 2015; Yao et al., 2014). Across the analyses, we identified large clusters of grey matter loss in regions associated with higher order visual processing (i.e., dorsal and ventral visual pathways) and the Default Mode Network (DMN), and specifically the precuneus, one of the DMN nodes, which is embedded in the parietal lobe and is involved in information processing (including visual information) (Buckner et al., 2008; Cavanna & Trimble, 2006; Freton et al., 2014; Hafkemeijer et al., 2012; Lenka et al., 2015). Grey matter volume loss in these areas may lead to dysfunctional information integration giving rise to visual hallucinations in PD patients, and also potentially due to an overreliance on endogenous attentional mechanisms (Shine et al., 2011; Shine, O'Callaghan, et al., 2014) as suggested by the involvement of DMN nodes (Rektorova et al., 2014).

Furthermore, this review expands on previous evidence by investigating the association between regional grey matter volume (as measured by Hedges' *g* effect-size estimates from the meta-analysis) and key candidate receptors involved in PDP as indexed by mRNA microarray gene expression extracted from the Allen Human Brain Atlas (Hawrylycz et al., 2012). Expression of 5-HT2a and 5-HT1a receptors were associated with estimates of grey matter volume, albeit being in opposite direction. Whether the inverse relationship observed here between pooled grey matter volume in PDP patients and the pooled expression of 5-HT2a

bioRxiv preprint doi: https://doi.org/10.1101/2022.11.14.516465; this version posted November 15, 2022. The copyright holder for this preprint (which was not certified by peer review) is the author/funder, who has granted bioRxiv a license to display the preprint in perpetuity. It is made available under aCC-BY-ND 4.0 International license.

receptors in an independent healthy cohort indicates that in PDP patients the greater the grey matter volume loss the greater is the regional 5-HT2a receptor availability, remains to be tested by direct investigation using both imaging modalities in the same group of participants. Nevertheless, if an association between grey matter loss in PDP and increased 5-HT2a receptor availability is demonstrated in PDP, it would be consistent with pharmacological evidence of the efficacy of the atypical antipsychotic Pimavanserin, a highly selective 5-HT2a receptor antagonist, in the treatment of psychosis in PD (Majlath et al., 2017; Meltzer et al., 2010; Mohanty et al., 2019; Stahl, 2016a; Yunusa et al., 2020). On the other hand, the direct relationship between grey matter volume and the pooled expression of 5-HT1a receptors, may indicate that in PDP patients the lower the grey matter volume the lower the regional availability of 5-HT1a receptors. Whether this holds true when investigated using both imaging modalities in the same cohort of patients remains to be seen. Given the association between 5-HT1a abnormalities and depression (Wang et al., 2016), this may reflect the common co-occurrence of depressive symptoms in people with PDP. While the degeneration of dopaminergic neurons in the substantia nigra is the hallmark of PD pathology, it is also followed by degeneration of serotonergic neurons in subcortical areas such as the raphe nuclei (Stahl, 2016b). Further, upregulation of 5-HT2a receptors has been observed in visual and temporal regions in PDP patients which may be a result of Lewy bodies accumulation in subcortical regions which also was associated with presence of hallucinatory behaviour (Birkmayer et al., 1974; Huot, 2018; Huot et al., 2010). Our results are in line with those from Vignando et al.'s (Vignando et al., 2021) analysis showing association between structural measures and 5-HT2a and 5-HT1a binding but not in terms of relationship with regional D1 density.

Presumably, the development of psychosis in PD patients could then be due to dysfunction in networks involved in attention control and visual information processing (Lenka et al., 2015; Muller et al., 2014; Shine, Halliday, et al., 2014; Shine et al., 2011; Shine, O'Callaghan, et al., 2014) that become pathological due to grey matter reduction in their nodes, as shown in the meta-analysis results, which consequently leads to abnormal functionality at a network level. Our results are to some extent different from those of the mega-analysis (Vignando et al., 2021) and may be due to the diverse methodologies used (mega-analysis vs. meta-analysis), the qualitative synthesis of multi-modal neuroimaging studies, the parameters used to assess atrophy (cortical thickness and surface area vs. voxel-based grey matter), and the availability of raw data (subject-level data vs. peak coordinates and one T map). They

bioRxiv preprint doi: https://doi.org/10.1101/2022.11.14.516465; this version posted November 15, 2022. The copyright holder for this preprint (which was not certified by peer review) is the author/funder, who has granted bioRxiv a license to display the preprint in perpetuity. It is made available under aCC-BY-ND 4.0 International license.

reported reduced surface area and extensive reduction in cortical thickness in occipital, temporal, parietal, frontal and limbic regions in PDP patients with visual hallucinations, identifying asymmetry in the left ventral visual pathway and extensive cortical thinning in bilateral cuneus, left dorso-medial superior frontal gyrus. Conversely, we mainly reported parietal-temporo-occipital regions as areas of significant grey matter loss and two frontal regions were found involved in PDP (the latter observed in the main analysis and in the analysis adjusted for cognitive state), our results however did not survive familywise error correction. Interestingly, we identified the right precuneus (extending to the left precuneus) as the largest cluster affected by grey matter loss in PDP patients across the three analyses (i.e., unadjusted, adjusted for PD medication and for cognition). The cuneus and precuneus were also reported as two of the areas with the greatest effect size in the principal component analysis by Vignando et al. (2021) examining the nodes that contributed the most to cortical thickness reduction in PDP patients, as well as in their network analysis. We conducted a whole-brain association between grey matter loss in PDP patients and receptor density examining dopaminergic and serotonergic receptors. We did not observe any relationships between grey matter volume and regional D1 density. This is in contrast with Vignando et al. (2021) who found associations with dopaminergic receptor density with cortical thickness in regions where PDP and PDnP had significant differences, and with surface area for significant regions of difference as well as across the cortex. However, we were only able to extract data on D1/D2 receptors unlike Vignando et al. (2021) who investigated the relationship with D2/D3 joint receptor density distribution. This discrepancy may also be due to methodological differences: they used mean thickness differences as the outcome variable, whilst we employed Hedges' *g* effect-size estimates extracted from SDM-PSI used as a measure of grey matter loss in PDP patients, lastly they examined in-vivo PET data from an independent healthy cohort whilst we relied on gene expression data extracted from six healthy donors of the Allen Human Brain Atlas (Arnatkevičiūtė et al., 2019; Desikan et al., 2006).

4.1. Strength and limitations

The main limitations were the lack of significant results in the family-wise error corrected analyses potentially due to the small number studies and the limited access to raw imaging data as we mainly relied on peak coordinates, a less powerful approach (Salimi-Khorshidi et al., 2009), and that we have fewer studies than recommended guidelines (Müller et al., 2018). We were also unable to relate meta-analytic estimates with psychotic symptoms. These studies focused on visual hallucinations in PD. This may also be due to the different

bioRxiv preprint doi: https://doi.org/10.1101/2022.11.14.516465; this version posted November 15, 2022. The copyright holder for this preprint (which was not certified by peer review) is the author/funder, who has granted bioRxiv a license to display the preprint in perpetuity. It is made available under aCC-BY-ND 4.0 International license.

rating scales applied to assess the presence of these symptoms, some measures may not differentiate or may not be sensitive to these symptoms. Whilst some studies referred to the NINDS-NIMH criteria (Ravina et al., 2007), most used different assessment tools or interviews. Although visual hallucinations and illusions are the most prevalent psychotic manifestations in PD, there is evidence of patients experiencing auditory and multimodal (e.g., olfactory, tactile (Chou et al., 2005; Solla et al., 2021)) hallucinations and delusions (Goetz et al., 2006; Marsh et al., 2004; Papapetropoulos et al., 2008) as the disease progresses, leading to increased distress and worsening of quality of life for the patients. Future exploration should compare the neuroanatomical correlates of different psychotic symptoms in PD, as this can shed light on whether there are common pathways shared with visual hallucinations, as those observed in this meta-analysis, or symptom-specific dysfunction. A further limitation is that we used mRNA expression, a result of transcriptional and translation activity, as a measure of dopaminergic (i.e., D1, D2) and serotonergic (i.e., 5-HT2a, 5-HT1a) gene expression extracted from 6 neurotypical donors (Hawrylycz et al., 2012) which may not be presentative of the PD population and may introduce variability due to inter-individual differences. Nevertheless, several studies employing this methodology have shown the consistency of the receptor spatial architecture in the cortex across individuals (Beliveau et al., 2017; Rizzo et al., 2016; Rizzo et al., 2014; Selvaggi et al., 2019; Veronese et al., 2016). Similar approaches have been applied by other studies assessing the relationship between estimates of brain functions (from fMRI studies) and regional gene expression data, also under pharmacological intervention (Anderson et al., 2020; Gryglewski et al., 2018; Richiardi et al., 2015; Selvaggi et al., 2019; Vértes et al.). Using mRNA expression data can pave the way in the use of different techniques, also more available to the wider community, to measure regional receptor expression in the whole brain when there is a paucity of in-vivo data.

4.2. Conclusions

In conclusion, there was grey matter volume loss in the parietal-temporal-occipital region which persisted even after adjusting for the effects of PD medications and cognitive scores. Although it may be premature to infer definite conclusions, the above evidence suggests that anomalies in brain regions involved in processing visual stimuli, over reliance on internal processing, and potential deficits in directing attention and integrating endogenous and externally derived information may underlie psychosis in PD. These findings relate to PD patients with mainly visual hallucinations due to the predominance of this symptom in the

bioRxiv preprint doi: https://doi.org/10.1101/2022.11.14.516465; this version posted November 15, 2022. The copyright holder for this preprint (which was not certified by peer review) is the author/funder, who has granted bioRxiv a license to display the preprint in perpetuity. It is made available under aCC-BY-ND 4.0 International license.

cohorts included in these studies. Furthermore, we observed an association between regional gene expression of serotonergic receptors and regional grey matter volume.

Acknowledgment: None

Authors' contributions:

Conceptualisation: Sara Pisani, Latha Velayudhan, Sagnik Bhattacharyya

Methodology: Sara Pisani, Brandon Gunasekera, Latha Velayudhan, Sagnik Bhattacharyya

Investigation: Sara Pisani, Latha Velayudhan, Sagnik Bhattacharyya

Data curation: Sara Pisani, Yining Lu

Formal analysis: Sara Pisani, Brandon Gunasekera, Yining Lu, Sagnik Bhattacharyya

Visualisation: Sarra Pisani, Sagnik Bhattacharyya

Funding acquisition: Sagnik Bhattacharyya, Latha Velayudhan, Dominic ffytche, Dag Aarsland, Kallol Ray Chaudhuri, Clive Ballard

Writing (original draft): Sara Pisani, Sagnik Bhattacharyya, Latha Velayudhan

Writing (review & editing): All authors

Supervision: Latha Velayudhan, Dominic ffytche, Sagnik Bhattacharyya

References

Aarsland, D., Brønnick, K., Ehrt, U., De Deyn, P. P., Tekin, S., Emre, M., & Cummings, J. L. (2007). Neuropsychiatric symptoms in patients with Parkinson's disease and dementia: frequency, profile and associated care giver stress. *J Neurol Neurosurg Psychiatry*, *78*(1), 36-42. https://doi.org/10.1136/jnnp.2005.083113

Albajes-Eizagirre, A., Solanes, A., & Radua, J. (2018). Meta-analysis of non-statistically significant unreported effects. *Statistical Methods in Medical Research*, *28*(12), 3741-3754. https://doi.org/10.1177/0962280218811349

Albajes-Eizagirre, A., Solanes, A., Vieta, E., & Radua, J. (2019). Voxel-based meta-analysis via permutation of subject images (PSI): theory and implementation for SDM. *Neuroimage*, *186*, 174-184.

Alzahrani, H., & Venneri, A. (2015). Cognitive and neuroanatomical correlates of neuropsychiatric symptoms in Parkinson's disease: A systematic review. *J Neurol Sci*, *356*(1-2), 32-44. https://doi.org/10.1016/j.jns.2015.06.037

Anderson, K. M., Collins, M. A., Chin, R., Ge, T., Rosenberg, M. D., & Holmes, A. J. (2020). Transcriptional and imaging-genetic association of cortical interneurons, brain function, and schizophrenia risk. *Nat Commun*, *11*(1), 2889. https://doi.org/10.1038/s41467-020-16710-x

Arnatkevičiūtė, A., Fulcher, B. D., & Fornito, A. (2019). A practical guide to linking brain-wide gene expression and neuroimaging data. *Neuroimage*, *189*, 353-367. https://doi.org/https://doi.org/10.1016/j.neuroimage.2019.01.011

Barrett, M. J., Blair, J. C., Sperling, S. A., Smolkin, M. E., & Druzgal, T. J. (2018). Baseline symptoms and basal forebrain volume predict future psychosis in early Parkinson disease. *Neurology*, *90*(18), e1618-e1626. https://doi.org/10.1212/wnl.0000000000005421

bioRxiv preprint doi: https://doi.org/10.1101/2022.11.14.516465; this version posted November 15, 2022. The copyright holder for this preprint (which was not certified by peer review) is the author/funder, who has granted bioRxiv a license to display the preprint in perpetuity. It is made available under aCC-BY-ND 4.0 International license.

Bejr-Kasem, H., Pagonabarraga, J., Martinez-Horta, S., Sampedro, F., Marin-Lahoz, J., Horta-Barba, A., Aracil-Bolanos, I., Perez-Perez, J., Boti, M. A., Campolongo, A., Izquierdo, C., Pascual-Sedano, B., Gomez-Anson, B., & Kulisevsky, J. (2019). Disruption of the default mode network and its intrinsic functional connectivity underlies minor hallucinations in Parkinson's disease [Article]. *Movement Disorders*, *34*(1), 78-86. https://doi.org/10.1002/mds.27557

Bejr-Kasem, H., Sampedro, F., Marín-Lahoz, J., Martínez-Horta, S., Pagonabarraga, J., & Kulisevsky, J. (2020). Minor hallucinations reflect early gray matter loss and predict subjective cognitive decline in parkinson's disease. *Eur J Neurol*. https://doi.org/10.1111/ene.14576

Beliveau, V., Ganz, M., Feng, L., Ozenne, B., Højgaard, L., Fisher, P. M., Svarer, C., Greve, D. N., & Knudsen, G. M. (2017). A High-Resolution In Vivo Atlas of the Human Brain's Serotonin System. *The Journal of Neuroscience*, *37*(1), 120. https://doi.org/10.1523/JNEUROSCI.2830-16.2016

Birkmayer, W., Danielczyk, W., Neumayer, E., & Riederer, P. (1974). Nucleus ruber and L-dopa psychosis: biochemical post-mortem findings. *J Neural Transm*, *35*(2), 93-116. https://doi.org/10.1007/bf01250738

Boecker, H., Ceballos-Baumann, A. O., Volk, D., Conrad, B., Forstl, H., & Haussermann, P. (2007). Metabolic alterations in patients with Parkinson disease and visual hallucinations. *Archives of Neurology*, *64*(7), 984-988.

Buckner, R. L., Andrews-Hanna, J. R., & Schacter, D. L. (2008). The Brain's Default Network. *Annals of the New York Academy of Sciences*, *1124*(1), 1-38. https://doi.org/https://doi.org/10.1196/annals.1440.011

Cavanna, A. E., & Trimble, M. R. (2006). The precuneus: a review of its functional anatomy and behavioural correlates. *Brain*, *129*(3), 564-583.

Chang, A., & Fox, S. H. (2016). Psychosis in Parkinson's Disease: Epidemiology, Pathophysiology, and Management. *Drugs*, *76*(11), 1093-1118. https://doi.org/10.1007/s40265-016-0600-5

Chou, K. L., Messing, S., Oakes, D., Feldman, P. D., Breier, A., & Friedman, J. H. (2005). Drug-induced psychosis in Parkinson disease - Phenomenology and correlations among psychosis rating instruments [Article; Proceedings Paper]. *Clinical Neuropharmacology*, *28*(5), 215-219. https://doi.org/10.1097/01.wnf.0000180228.77802.32

Desikan, R. S., Ségonne, F., Fischl, B., Quinn, B. T., Dickerson, B. C., Blacker, D., Buckner, R. L., Dale, A. M., Maguire, R. P., Hyman, B. T., Albert, M. S., & Killiany, R. J. (2006). An automated labeling system for subdividing the human cerebral cortex on MRI scans into gyral based regions of interest. *Neuroimage*, *31*(3), 968-980. https://doi.org/10.1016/j.neuroimage.2006.01.021

Egger, M., Davey Smith, G., Schneider, M., & Minder, C. (1997). Bias in meta-analysis detected by a simple, graphical test. *Bmj*, *315*(7109), 629-634. https://doi.org/10.1136/bmj.315.7109.629

Factor, S. A., Scullin, M. K., Sollinger, A. B., Land, J. O., Wood-Siverio, C., Zanders, L., Freeman, A., Bliwise, D. L., McDonald, W. M., & Goldstein, F. C. (2014). Cognitive correlates of hallucinations and delusions in Parkinson's disease. *J Neurol Sci*, *347*(1-2), 316-321. https://doi.org/10.1016/j.jns.2014.10.033

Ffytche, D. H., Creese, B., Politis, M., Chaudhuri, K. R., Weintraub, D., Ballard, C., & Aarsland, D. (2017). The psychosis spectrum in Parkinson disease. *Nat Rev Neurol*, *13*(2), 81-95. https://doi.org/10.1038/nrneurol.2016.200

Firbank, M. J., Parikh, J., Murphy, N., Killen, A., Allan, C. L., Collerton, D., Blamire, A. M., & Taylor, J.-P. (2018). Reduced occipital GABA in Parkinson disease with visual hallucinations. *Neurology*, *91*(7), e675. https://doi.org/10.1212/WNL.0000000000006007

Freton, M., Lemogne, C., Bergouignan, L., Delaveau, P., Lehéricy, S., & Fossati, P. (2014). The eye of the self: precuneus volume and visual perspective during autobiographical memory retrieval. *Brain Structure and Function*, *219*(3), 959-968. https://doi.org/10.1007/s00429-013-0546-2

Friedman, J. H. (2016). Minor hallucinations occur in drug-naive Parkinson's disease patients even from the premotor phase (vol 31, pg 9, 2016) [Correction]. *Movement Disorders*, *31*(3), 433-433. https://doi.org/10.1002/mds.26603

Gama, R. L., Bruin, V. M., Távora, D. G., Duran, F. L., Bittencourt, L., & Tufik, S. (2014). Structural brain abnormalities in patients with Parkinson's disease with visual hallucinations: a

bioRxiv preprint doi: https://doi.org/10.1101/2022.11.14.516465; this version posted November 15, 2022. The copyright holder for this preprint (which was not certified by peer review) is the author/funder, who has granted bioRxiv a license to display the preprint in perpetuity. It is made available under aCC-BY-ND 4.0 International license.

comparative voxel-based analysis. *Brain Cogn*, *87*, 97-103. https://doi.org/10.1016/j.bandc.2014.03.011

Goetz, C. G., Wuu, J., Curgian, L., & Leurgans, S. (2006). Age-related influences on the clinical characteristics of new-onset hallucinations in Parkinson's disease patients. *Movement Disorders*, *21*(2), 267-270.

Goldman, J. G., Stebbins, G. T., Dinh, V., Bernard, B., Merkitch, D., deToledo-Morrell, L., & Goetz, C. G. (2014). Visuoperceptive region atrophy independent of cognitive status in patients with Parkinson's disease with hallucinations. *Brain*, *137*(3), 849-859.

Gryglewski, G., Seiger, R., James, G. M., Godbersen, G. M., Komorowski, A., Unterholzner, J., Michenthaler, P., Hahn, A., Wadsak, W., Mitterhauser, M., Kasper, S., & Lanzenberger, R. (2018). Spatial analysis and high resolution mapping of the human whole-brain transcriptome for integrative analysis in neuroimaging. *Neuroimage*, *176*, 259-267. https://doi.org/https://doi.org/10.1016/j.neuroimage.2018.04.068

Hacksell, U., Burstein, E. S., McFarland, K., Mills, R. G., & Williams, H. (2014). On the discovery and development of pimavanserin: a novel drug candidate for Parkinson's psychosis. *Neurochemical research*, *39*(10), 2008-2017.

Hafkemeijer, A., van der Grond, J., & Rombouts, S. A. R. B. (2012). Imaging the default mode network in aging and dementia. *Biochimica et Biophysica Acta (BBA) - Molecular Basis of Disease*, *1822*(3), 431-441. https://doi.org/https://doi.org/10.1016/j.bbadis.2011.07.008

Hall, J. M., O'Callaghan, C., Muller, A. J., Martens, K. A. E., Phillips, J. R., Moustafa, A. A., Lewis, S. J. G., & Shine, J. M. (2019). Changes in structural network topology correlate with severity of hallucinatory behavior in Parkinson's disease [Article]. *Network Neuroscience*, *3*(2), 521-538. https://doi.org/10.1162/netn_a_00078

Hawrylycz, M. J., Lein, E. S., Guillozet-Bongaarts, A. L., Shen, E. H., Ng, L., Miller, J. A., van de Lagemaat, L. N., Smith, K. A., Ebbert, A., Riley, Z. L., Abajian, C., Beckmann, C. F., Bernard, A., Bertagnolli, D., Boe, A. F., Cartagena, P. M., Chakravarty, M. M., Chapin, M., Chong, J., . . . Jones, A. R. (2012). An anatomically comprehensive atlas of the adult human brain transcriptome. *Nature*, *489*(7416), 391-399. https://doi.org/10.1038/nature11405

Hepp, D. H., Foncke, E. M. J., Berendse, H. W., Wassenaar, T. M., Dubbelink, K., Groenewegen, H. J., van de Berg, W. D. J., & Schoonheim, M. M. (2017). Damaged fiber tracts of the nucleus basalis of Meynert in Parkinson's disease patients with visual hallucinations [Article]. *Scientific Reports*, *7*. https://doi.org/10.1038/s41598-017-10146-y

Higgins, J. P., Thompson, S. G., Deeks, J. J., & Altman, D. G. (2003). Measuring inconsistency in meta-analyses. *Bmj*, *327*(7414), 557-560. https://doi.org/10.1136/bmj.327.7414.557

Huot, P. (2018). 5-HT(2A) receptors and Parkinson's disease psychosis: a pharmacological discussion. *Neurodegener Dis Manag*, *8*(6), 363-365. https://doi.org/10.2217/nmt-2018-0039

Huot, P., Johnston, T. H., Darr, T., Hazrati, L. N., Visanji, N. P., Pires, D., Brotchie, J. M., & Fox, S. H. (2010). Increased 5-HT<inf>2A</inf> receptors in the temporal cortex of Parkinsonian patients with visual hallucinations. *Movement Disorders*, *25*(10), 1399-1408. https://doi.org/http://dx.doi.org/10.1002/mds.23083

Jia, X., Li, Y., Li, K., Liang, P., & Fu, X. (2019). Precuneus dysfunction in Parkinson's disease with mild cognitive impairment. *Frontiers in aging neuroscience*, *10*, 427.

Lawn, T. (2021). Cerebellar correlates of visual hallucinations in Parkinson's disease and Charles Bonnet Syndrome. *Cortex*, *135*, 311-325.

Lee, W. W., Yoon, E. J., Lee, J. Y., Park, S. W., & Kim, Y. K. (2017). Visual Hallucination and Pattern of Brain Degeneration in Parkinsons Disease [Article]. *Neurodegenerative Diseases*, *17*(2-3), 63-72. https://doi.org/10.1159/000448517

Lefebvre, S., Baille, G., Jardri, R., Plomhause, L., Szaffarczyk, S., Defebvre, L., Thomas, P., Delmaire, C., Pins, D., & Dujardin, K. (2016). Hallucinations and conscious access to visual inputs in Parkinson's disease. *Scientific Reports*, *6*(1), 36284. https://doi.org/10.1038/srep36284

Lenka, A., Jhunjhunwala, K. R., Saini, J., & Pal, P. K. (2015). Structural and functional neuroimaging in patients with Parkinson's disease and visual hallucinations: A critical review. *Parkinsonism Relat Disord*, *21*(7), 683-691. https://doi.org/10.1016/j.parkreldis.2015.04.005

bioRxiv preprint doi: https://doi.org/10.1101/2022.11.14.516465; this version posted November 15, 2022. The copyright holder for this preprint (which was not certified by peer review) is the author/funder, who has granted bioRxiv a license to display the preprint in perpetuity. It is made available under aCC-BY-ND 4.0 International license.

Luo, D., Wan, X., Liu, J., & Tong, T. (2018). Optimally estimating the sample mean from the sample size, median, mid-range, and/or mid-quartile range. *Stat Methods Med Res*, *27*(6), 1785-1805. https://doi.org/10.1177/0962280216669183

Majlath, Z., Obal, I., & Vecsei, L. (2017). Treatment Possibilities for Psychosis in Parkinson's Disease with An Emphasis on the Newly Approved Drug: Pimavanserin. *CNS Neurol Disord Drug Targets*, *16*(3), 234-243. https://doi.org/10.2174/1871527315666161006104347

Markello, R. D., Arnatkeviciute, A., Poline, J. B., Fulcher, B. D., Fornito, A., & Misic, B. (2021). Standardizing workflows in imaging transcriptomics with the abagen toolbox. *Elife*, *10*. https://doi.org/10.7554/eLife.72129

Marsh, L., Williams, J. R., Rocco, M., Grill, S., Munro, C., & Dawson, T. M. (2004). Psychiatric comorbidities in patients with Parkinson disease and psychosis. *Neurology*, *63*(2), 293-300. https://doi.org/10.1212/01.wnl.0000129843.15756.a3

Martinez-Martin, P., Rodriguez-Blazquez, C., Forjaz, M. J., Frades-Payo, B., Agüera-Ortiz, L., Weintraub, D., Riesco, A., Kurtis, M. M., & Chaudhuri, K. R. (2015). Neuropsychiatric symptoms and caregiver's burden in Parkinson's disease. *Parkinsonism Relat Disord*, *21*(6), 629-634. https://doi.org/10.1016/j.parkreldis.2015.03.024

Meltzer, H. Y., Mills, R., Revell, S., Williams, H., Johnson, A., Bahr, D., & Friedman, J. H. (2010). Pimavanserin, a serotonin(2A) receptor inverse agonist, for the treatment of parkinson's disease psychosis. *Neuropsychopharmacology*, *35*(4), 881-892. https://doi.org/10.1038/npp.2009.176

Mohanty, D., Sarai, S., Naik, S., & Lippmann, S. (2019). Pimavanserin for Parkinson Disease Psychosis. *Prim Care Companion CNS Disord*, *21*(2). https://doi.org/10.4088/PCC.18l02355

Moher, D., Liberati, A., Tetzlaff, J., Altman, D. G., & The, P. G. (2009). Preferred Reporting Items for Systematic Reviews and Meta-Analyses: The PRISMA Statement. *PLOS Medicine*, *6*(7), e1000097. https://doi.org/10.1371/journal.pmed.1000097

Muller, A. J., Shine, J. M., Halliday, G. M., & Lewis, S. J. (2014). Visual hallucinations in Parkinson's disease: theoretical models. *Movement Disorders*, *29*(13), 1591-1598.

Müller, V. I., Cieslik, E. C., Laird, A. R., Fox, P. T., Radua, J., Mataix-Cols, D., Tench, C. R., Yarkoni, T., Nichols, T. E., Turkeltaub, P. E., Wager, T. D., & Eickhoff, S. B. (2018). Ten simple rules for neuroimaging meta-analysis. *Neuroscience & Biobehavioral Reviews*, *84*, 151-161. https://doi.org/https://doi.org/10.1016/j.neubiorev.2017.11.012

Nishio, Y., Yokoi, K., Hirayama, K., Ishioka, T., Hosokai, Y., Gang, M., Uschiyama, M., Baba, T., Suzuki, K., Takeda, A., & Mori, E. (2018). Defining visual illusions in Parkinson's disease: Kinetopsia and object misidentification illusions. *Parkinsonism & related disorders*, *55*, 111-116. https://doi.org/10.1016/j.parkreldis.2018.05.023

Pagonabarraga, J., Martinez-Horta, S., Fernández de Bobadilla, R., Pérez, J., Ribosa-Nogué, R., Marín, J., Pascual-Sedano, B., García, C., Gironell, A., & Kulisevsky, J. (2016). Minor hallucinations occur in drug-naive Parkinson's disease patients, even from the premotor phase. *Mov Disord*, *31*(1), 45-52. https://doi.org/10.1002/mds.26432

Pagonabarraga, J., Soriano-Mas, C., Llebaria, G., López-Solà, M., Pujol, J., & Kulisevsky, J. (2014). Neural correlates of minor hallucinations in non-demented patients with Parkinson's disease. *Parkinsonism & Related Disorders*, *20*(3), 290-296.

Papapetropoulos, S., Katzen, H., Schrag, A., Singer, C., Scanlon, B. K., Nation, D., Guevara, A., & Levin, B. (2008). A questionnaire-based (UM-PDHQ) study of hallucinations in Parkinson's disease. *BMC neurology*, *8*(1), 1-8.

Pezzoli, S., Sánchez-Valle, R., Solanes, A., Kempton, M. J., Bandmann, O., Shin, J. I., Cagnin, A., Goldman, J. G., Merkitch, D., & Firbank, M. J. (2021). Neuroanatomical and cognitive correlates of visual hallucinations in Parkinson's disease and dementia with Lewy bodies: voxel-based morphometry and neuropsychological meta-analysis. *Neuroscience & Biobehavioral Reviews*, *128*, 367-382.

Ramírez-Ruiz, B., Martí, M. J., Tolosa, E., Gimenez, M., Bargallo, N., Valldeoriola, F., & Junque, C. (2007). Cerebral atrophy in Parkinson's disease patients with visual hallucinations. *European Journal of Neurology*, *14*(7), 750-756.

Ravina, B., Marder, K., Fernandez, H. H., Friedman, J. H., McDonald, W., Murphy, D., Aarsland, D., Babcock, D., Cummings, J., & Endicott, J. (2007). Diagnostic criteria for psychosis in

bioRxiv preprint doi: https://doi.org/10.1101/2022.11.14.516465; this version posted November 15, 2022. The copyright holder for this preprint (which was not certified by peer review) is the author/funder, who has granted bioRxiv a license to display the preprint in perpetuity. It is made available under aCC-BY-ND 4.0 International license.

Parkinson's disease: report of an NINDS, NIMH work group. *Movement Disorders*, *22*(8), 1061-1068.

Rektorova, I., Krajcovicova, L., Marecek, R., Novakova, M., & Mikl, M. (2014). Default Mode Network Connectivity Patterns associated with Visual Processing at Different Stages of Parkinson's Disease. *Journal of Alzheimers Disease*, *42*, S217-S228. https://doi.org/10.3233/jad-132684

Richiardi, J., Altmann, A., Milazzo, A.-C., Chang, C., Chakravarty, M. M., Banaschewski, T., Barker, G. J., Bokde, A. L. W., Bromberg, U., Büchel, C., Conrod, P., Fauth-Bühler, M., Flor, H., Frouin, V., Gallinat, J., Garavan, H., Gowland, P., Heinz, A., Lemaître, H., . . . Tahmasebi, A. (2015). Correlated gene expression supports synchronous activity in brain networks. *Science*, *348*(6240), 1241-1244. https://doi.org/10.1126/science.1255905

Rizzo, G., Veronese, M., Expert, P., Turkheimer, F. E., & Bertoldo, A. (2016). MENGA: A New Comprehensive Tool for the Integration of Neuroimaging Data and the Allen Human Brain Transcriptome Atlas. *PLoS One*, *11*(2), e0148744. https://doi.org/10.1371/journal.pone.0148744

Rizzo, G., Veronese, M., Heckemann, R. A., Selvaraj, S., Howes, O. D., Hammers, A., Turkheimer, F. E., & Bertoldo, A. (2014). The Predictive Power of Brain mRNA Mappings for in vivo Protein Density: A Positron Emission Tomography Correlation Study. *Journal of Cerebral Blood Flow & Metabolism*, *34*(5), 827-835. https://doi.org/10.1038/jcbfm.2014.21

Salimi-Khorshidi, G., Smith, S. M., Keltner, J. R., Wager, T. D., & Nichols, T. E. (2009). Meta-analysis of neuroimaging data: A comparison of image-based and coordinate-based pooling of studies. *Neuroimage*, *45*(3), 810-823. https://doi.org/https://doi.org/10.1016/j.neuroimage.2008.12.039

Selvaggi, P., Hawkins, P. C. T., Dipasquale, O., Rizzo, G., Bertolino, A., Dukart, J., Sambataro, F., Pergola, G., Williams, S. C. R., Turkheimer, F., Zelaya, F., Veronese, M., & Mehta, M. A. (2019). Increased cerebral blood flow after single dose of antipsychotics in healthy volunteers depends on dopamine D2 receptor density profiles. *Neuroimage*, *188*, 774-784. https://doi.org/10.1016/j.neuroimage.2018.12.028

Shin, S., Lee, J. E., Hong, J. Y., Sunwoo, M.-K., Sohn, Y. H., & Lee, P. H. (2012). Neuroanatomical substrates of visual hallucinations in patients with non-demented Parkinson's disease. *Journal of neurology, neurosurgery & psychiatry*, *83*(12), 1155-1161.

Shine, J. M., Halliday, G. M., Gilat, M., Matar, E., Bolitho, S. J., Carlos, M., Naismith, S. L., & Lewis, S. J. (2014). The role of dysfunctional attentional control networks in visual misperceptions in Parkinson's disease. *Human Brain Mapping*, *35*(5), 2206-2219.

Shine, J. M., Halliday, G. M., Naismith, S. L., & Lewis, S. J. G. (2011). Visual Misperceptions and Hallucinations in Parkinson's Disease: Dysfunction of Attentional Control Networks? [Article]. *Movement Disorders*, *26*(12), 2154-2159. https://doi.org/10.1002/mds.23896

Shine, J. M., Keogh, R., O'Callaghan, C., Muller, A. J., Lewis, S. J. G., & Pearson, J. (2015). Imagine that: elevated sensory strength of mental imagery in individuals with Parkinson's disease and visual hallucinations [Article]. *Proceedings of the Royal Society B-Biological Sciences*, *282*(1798). https://doi.org/10.1098/rspb.2014.2047

Shine, J. M., O'Callaghan, C., Halliday, G. M., & Lewis, S. J. (2014). Tricks of the mind: visual hallucinations as disorders of attention. *Progress in neurobiology*, *116*, 58-65.

Solla, P., Masala, C., Pinna, I., Ercoli, T., Loy, F., Orofino, G., Fadda, L., & Defazio, G. (2021). Frequency and Determinants of Olfactory Hallucinations in Parkinson's Disease Patients. *Brain sciences*, *11*(7), 841. https://doi.org/10.3390/brainsci11070841

Stahl, S. M. (2016a). Mechanism of action of pimavanserin in Parkinson's disease psychosis: targeting serotonin 5HT2A and 5HT2C receptors. *CNS Spectr*, *21*(4), 271-275. https://doi.org/10.1017/s1092852916000407

Stahl, S. M. (2016b). Parkinson's disease psychosis as a serotonin-dopamine imbalance syndrome. *CNS Spectr*, *21*(5), 355-359. https://doi.org/10.1017/s1092852916000602

Stebbins, G. T., Goetz, C. G., Carrillo, M. C., Bangen, K. J., Turner, D. A., Glover, G. H., & Gabrieli, J. D. E. (2004). Altered cortical visual processing in PD with hallucinations - An fMRI study [Article]. *Neurology*, *63*(8), 1409-1416.

bioRxiv preprint doi: https://doi.org/10.1101/2022.11.14.516465; this version posted November 15, 2022. The copyright holder for this preprint (which was not certified by peer review) is the author/funder, who has granted bioRxiv a license to display the preprint in perpetuity. It is made available under aCC-BY-ND 4.0 International license.

Veronese, M., Zanotti-Fregonara, P., Rizzo, G., Bertoldo, A., Innis, R. B., & Turkheimer, F. E. (2016). Measuring specific receptor binding of a PET radioligand in human brain without pharmacological blockade: The genomic plot. *Neuroimage*, *130*, 1-12. https://doi.org/https://doi.org/10.1016/j.neuroimage.2016.01.058

Vértes, P. E., Rittman, T., Whitaker, K. J., Romero-Garcia, R., Váša, F., Kitzbichler, M. A.-O., Wagstyl, K., Fonagy, P., Dolan, R. J., Jones, P. B., Goodyer, I. M., & Bullmore, E. A.-O. Gene transcription profiles associated with inter-modular hubs and connection distance in human functional magnetic resonance imaging networks. LID - 10.1098/rstb.2015.0362 [doi] LID - 20150362. (1471-2970 (Electronic)).

Vignando, M., ffytche, D., Lewis, S., Lee, P. H., Chung, S. J., Weil, R. S., Hu, M. T., Mackay, C. E., Griffanti, L., Pins, D., Dujardin, K., Jardri, R., Taylor, J.-P., Firbank, M., McAlonan, G., Mak, H. K.-F., Ho, S. L., & Mehta, M. A. (2021). Mapping brain structural differences and neuroreceptor correlates in Parkinson's disease visual hallucinations: a mega-analysis. *medRxiv*, 2021.2002.2017.21251558. https://doi.org/10.1101/2021.02.17.21251558

Wang, L., Zhou, C., Zhu, D., Wang, X., Fang, L., Zhong, J., Mao, Q., Sun, L., Gong, X., Xia, J., Lian, B., & Xie, P. (2016). Serotonin-1A receptor alterations in depression: a meta-analysis of molecular imaging studies. *BMC Psychiatry*, *16*(1), 319. https://doi.org/10.1186/s12888-016-1025-0

Watanabe, H., Senda, J., Kato, S., Ito, M., Atsuta, N., Hara, K., Tsuboi, T., Katsuno, M., Nakamura, T., & Hirayama, M. (2013). Cortical and subcortical brain atrophy in Parkinson's disease with visual hallucination. *Movement Disorders*, *28*(12), 1732-1736.

Wells, G. A., Shea, B., O'Connell, D., Peterson, J., Welch, V., Losos, M., & Tugwell, P. (2000). The Newcastle-Ottawa Scale (NOS) for assessing the quality of nonrandomised studies in meta-analyses. In: Oxford.

Williams, D. R., & Lees, A. J. (2005). Visual hallucinations in the diagnosis of idiopathic Parkinson's disease: a retrospective autopsy study. *Lancet Neurol*, *4*(10), 605-610. https://doi.org/10.1016/s1474-4422(05)70146-0

Yao, N. L., Chang, R. S. K., Cheung, C., Pang, S., Lau, K. K., Suckling, J., Rowe, J. B., Yu, K., Mak, H. K. F., Chua, S. E., Ho, S. L., & McAlonan, G. M. (2014). The Default Mode Network is Disrupted in Parkinson's Disease with Visual Hallucinations [Article]. *Human Brain Mapping*, *35*(11), 5658-5666. https://doi.org/10.1002/hbm.22577

Yao, N. L., Cheung, C., Pang, S., Chang, R. S. K., Lau, K. K., Suckling, J., Yu, K., Mak, H. K. F., Chua, S. E., Ho, S. L., & McAlonan, G. M. (2016). Multimodal MRI of the hippocampus in Parkinson's disease with visual hallucinations [Article]. *Brain Structure & Function*, *221*(1), 287-300. https://doi.org/10.1007/s00429-014-0907-5

Yunusa, I., El Helou, M. L., & Alsahali, S. (2020). Pimavanserin: A Novel Antipsychotic With Potentials to Address an Unmet Need of Older Adults With Dementia-Related Psychosis [Mini Review]. *Frontiers in Pharmacology*, *11*. https://doi.org/10.3389/fphar.2020.00087